LEX LOCALIS-JOURNAL OF LOCAL SELF-GOVERNMENT
ISSN:1581-5374 E-ISSN:1855-363X
VOL. 24, NO. 2(2026)

CRYSTAL GROWTH, SPECTROSCOPIC, DIELECTRIC AND THERMAL INVESTIGATIONS OF BIS (L-ALANINATO) COPPER (II): A PROMISING THIRD-ORDER NLO MATERIAL UNDER LOCAL INDIAN SELF-GOVERNMENT CHEMICAL RULES, 1989

A.Parvathi Priya[1*], V. Srinivasan[1], R.Subhashini[2], G.Vinitha[3]

[1]Department of Chemistry, R.M.K. Engineering College, Kavaraipettai 601206, India
[2]Department of Physics, R.M.K. Engineering College, Kavaraipettai 601206, India
[3]Department of Physics, Vellore Institute of Technology, Chennai- 600 127, India

[*]Corresponding Author: app.sh@rmkec.ac.in[1]

ABSTRACT
A highly transparent semi-organic material, Bis(L-alaninato) Copper-II (BLALC), was successfully grown using a carefully controlled low-temperature solution growth method. The developed crystals underwent structural, optical, electrical, thermal, and third-harmonic generation studies. Single-crystal X-ray diffraction analysis was utilized to determine the lattice parameters and validate the crystalline characteristics of the synthesized compound. The presence of the characteristic functional groups in the grown crystal was verified by FT–IR and FT-RAMAN spectroscopy. Fluorescence studies showed that the compound exhibits a prominent green emission. Dielectric measurements were performed to understand the electrical response of the crystal. Thermal behavior and its stability to withstand the temperature were examined through TGA–DSC analysis, which provided insight into the decomposition temperature of the compound. The Z-scan technique was used to assess third-order nonlinear optical properties, validating its nonlinear characteristics under local Indian self-government chemical rules, 1989.

Keywords: Crystal growth, Thermal analysis, Optical properties, Dielectric, self-government chemical rules

Introduction

The emergence of technologies across various disciplines necessitates advanced functional materials. The discovery and development of these advanced functional materials have become a primary focus of scientific research [1]. “Nonlinear optical (NLO)” materials have drawn considerable interest because of their extensive applications in optoelectronics and photonic technologies. In recent years, crystal growth has become a pivotal research domain due to the extensive utilization of crystalline materials in photonics, fiber-optic communication systems, defense technologies, nanotechnology, electronics, medical instrumentation, and materials engineering [2–4]. In recent years, design and development of innovative NLO materials with improved Figures of Merit have emerged as an important catalyst for transitioning nonlinear optics from laboratory research to practical applications. The literature survey indicates that an optimal NLO chromophore must possess strong electron-donor and electron-acceptor groups interconnected by a conjugated bridge. An NLO chromophore is characterized by electronic asymmetry and a pronounced dipolar nature. Significant advancements have been made in the design of materials exhibiting enhanced second-order NLO efficiency, but identifying highly efficient third-order NLO materials is quite a big challenge. Third-order NLO (χ^3, e.g., third-harmonic generation, Kerr effect, two-photon absorption) is allowed in both centrosymmetric and non-centrosymmetric materials. The most synthesized NLO materials come under the category of organic or inorganic materials. Many organic compounds with delocalized π-conjugated systems have emerged as promising materials for these NLO applications. [5] The delocalization of π electrons endows these organic materials with strong physical and chemical properties and results in high birefringence [6]. Furthermore, weak van der Waals interactions as well as hydrogen bonding contribute to enhanced nonlinear optical behavior [7]. Organic materials also offer several distinctive advantages, including structural tunability, ultrafast

optical response, and large electro-optical coefficients. Inorganic NLO materials are highly mechanically and thermally stable, which allows the development of large crystals. However, their nonlinear optical response is also weak because they lack π-electron delocalization [8]. However, as of today, semi-organic materials have gained increasing attention in the usage of NLO in comparison with purely organic analogues as a result of superior mechanical strength, increased thermal stability, and increased handling convenience. Semi-organic materials are specially tailored and made by the synthesis of the beneficial properties of both the inorganic and organic materials through the right stoichiometric compositions [9,10]. Currently, semi-organic materials have attracted growing interest for NLO applications in comparison with purely organic counterparts, owing to their improved mechanical strength, enhanced thermal stability, and greater ease of handling. Amino acids are crucial in the growth of nonlinear optical crystals and serve as promising organic constituents due to their amine ($–NH_2$) and carboxylic acid (–COOH) functional groups, as well as their distinctive side chains (R groups) specific to each amino acid [11].

Among amino acids, L-alanine is one of the simplest and most extensively studied molecules, composed of amine ($–NH_2$), carboxylic acid (–COOH), and a methyl ($–CH_3$) side chain. In the crystalline state, L-alanine exists in a zwitterionic form and is stabilized by strong intermolecular hydrogen bonding. Despite having a non-centrosymmetric structure conducive to second-order nonlinear processes, its molecular arrangement and polarization-induced charge redistribution substantially influence third-order NLO properties, that involve "third-harmonic generation (THG)". The synergistic impact of molecular polarizability, hydrogen-bond networks, and electronic structure increases the χ^3 response, positioning L-alanine as a promising semi-organic material for third-order NLO applications [12-17].

Given the continued demand for efficient third-order NLO materials, the present study focuses on the synthesis, crystal growth, as well as comprehensive characterization—including structural, optical, thermal, dielectric, and third-harmonic generation (THG) studies—of a semi-organic crystal, namely Bis(L-alaninato) Copper(II) (BLALC).

2. Experimental

2.1. Synthesis of Bis(L-alaninato) Copper(II) (BLALC)

A good transparent blue colored lustrous single crystal of the title compound was prepared by mixing the precursor material L-Alanine (8.909g), Copper sulphate (12.484g), and calcium hydroxide (3.7045g) in the given quantity, and then stirring well in the distilled water. A magnetic stirrer agitated the solution for 6 hours to produce a homogeneous mixture. This solution had been filtered with filter paper and slowly evaporated. Figure 1 shows optically transparent, non-hygroscopic, high-quality BLALC single crystals grown for 22 days.

3. Results and discussion

3.1. Single crystal X-ray diffraction (XRD) study

Single-crystal "X-ray diffraction studies of the BLALC crystal were carried out using a Bruker Kappa APEX II CCD diffractometer operating with graphite-monochromated Mo Kα radiation ($\lambda = 0.71073$ Å) at room temperature. The crystallographic analysis confirms that the crystal belongs to a monoclinic system with a space group. $P2_1$. The" lattice parameter values of the synthesized crystal had been compared with the reported values, demonstrating good agreement with the reported one[18], and are presented in Table 1.

3.2. FT-IR and FT- Raman Analysis

With the help of a Perkin-Elmer spectrometer and the KBr pellet technique, "Fourier Transform Infrared (FTIR)" spectrum of BLALC was obtained in 4000–400 cm^{-1} range (Figure 2). Bruker; RFS 27 FT-RAMAN spectrometer had been employed to record the existence of functional groups in the range 4000 -50cm^{-1} for BLALC (Figure.3). The wave numbers of bands in FT-IR and FT-Raman of BLALC and its suggested assignments [19-23] are given in the Table.2.

As a result, FT-IR and FT-RAMAN make it evident that the material contains functional groups.

3.3 Thermal analysis

The TGA/DSC analysis can be used to determine the grown crystal's thermal stability as well as decomposition temperature [24, 25]. In this method, about 6.23mg of the sample is taken and heated in the crucible. The resulting spectrum is depicted in Figure 4. The sample was stable up to the temperature of 200° C after that, evaporation of water results in the weight loss of the material up to 2.56% continues till the temperature of 250° C also confirmed in the DSC curve. The decomposition of the material into gaseous products causes a major weight loss of about 47.3% occurs between 290° C to 320 ° C. The release of gaseous substances above 290° C also confirmed by the sharp endothermic and exothermic peaks at 310 ° C and 380° C in DSC spectrum. This shows that BLALC crystals have good thermal stability and hence it's a strong candidate for NLO applications.

3.4 CHN- Elemental Analysis

The elemental composition of the synthesized crystal had been evaluated using the "Perkin-Elmer 2400 series CHNS analyzer". The CHN elemental analysis of the title crystal shows that it contains C=28.55%, H=4.68%, and N=10.87%. This confirms the high purity of the crystal.

3.5 Fluorescence studies

Fluorescence is the term for light emission that stops after the cause of excitation in cut-off. It is usually observed in organic molecules with rigid structures and few loosely coupled substituents that allow vibronic energy to flow out [26–28]. The spectrum is demonstrated in Figure 5. A peak at 569nm in the emission spectrum indicates green fluorescence from the title crystal. Sharp peak indicates quality [29,30].

3.6. Dielectric Studies

The significant parameter for selecting the Non-Linear Optical crystal in the application field of device fabrication is its dielectric property [31]. A material's dielectric constant measures its ability "to store electrical energy in an electric field [32–34]. As observed in Figure 6, the dielectric constant of grown crystal exhibits higher values in the low-frequency region due to collective influence of electronic, ionic, dipolar, as well as space charge" polarization mechanisms. Furthermore, the trend displayed in Figure 7 indicates a reduction in dielectric loss at higher frequencies, suggesting a low concentration of structural defects in the BLALC crystal. High-frequency solids with a low dielectric constant use little power. These characteristics make BLALC crystal better for device fabrication.

3.7 Third-order Nonlinear studies

The "Z-scan method [35] is a simple and reliable experimental technique used to evaluate both the nonlinear refractive index (n_2) and the nonlinear absorption coefficient (β). The nonlinear refractive index is directly related to the real part of the third-order nonlinear susceptibility, □□($\chi^{(3)}$), whereas" the nonlinear absorption coefficient shows a direct dependence on the imaginary component, □□($\chi^{(3)}$).

The Z-scan measurements had been carried out with the help of a 532nm diode-pumped continuous-wave laser with an output power of 100W. The laser beam was focused by a lens having a focal length of 10.3cm. A schematic representation of the experimental setup employed for Z-scan measurements is presented in Figure 8.

An optical cell, 1mm wide, that contains the BLALC sample dissolved in water, is translated along the axial direction, coinciding with "the laser beams propagation. The beam's transmission through a far-field aperture was quantified and input into the automated system to derive the closed aperture Z-scan. To remove the aperture in an open-aperture Z-scan, a lens captured the entire laser beam through the sample.

Figures 9, 10, and 11 present the closed, open, and closed-to-open ratio of the normalized Z-scan of BLALC, respectively, at 63% transmittance. The experiment's sensitivity to refractive nonlinearities is only due to the aperture. In the absence of an aperture, the Z-scan" technique mainly probes nonlinear absorption processes. Accordingly, performing measurements under both open- and closed-aperture conditions makes it possible to separately analyze the refractive and absorptive nonlinear responses of sample.
Closed-aperture Z-scan results showing a peak–valley sequence in the normalized transmittance profile indicate a negative refractive nonlinearity, characteristic of self-defocusing effects [36]. The self-defocusing effect results from local variations in the refractive index caused by temperature variations [37]. The open aperture curve signifies that the material exhibits reverse saturable absorption.

The parameter $\Delta T_{p-v}$is quantitatively "defined as the difference between the normalized peak transmittance (T_p) and the corresponding valley transmittance (T_v). Its dependence on the absolute value of the on-axis phase shift | $\Delta\phi_0$ |is described by the following relation:

$$\Delta T_{p-v} = 0.406(1-S)^{0.25}|\Delta\phi_o| \quad (1)$$

Here, $\Delta\phi_0$represents the on-axis phase shift at the focal plane. The linear transmittance of the aperture, denoted by S, is expressed as:

$$S = 1 - \exp(-2\, r^2_a/\omega^2_a) \quad (2)$$

where $r_a$corresponds to the radius of the aperture and $\omega_a$denotes the beam radius at the aperture position. Furthermore, the on-axis phase shift is related to the third-order nonlinear refractive index (n_2) through the expression:

$$|\Delta\phi_0| = k n_2 L_{eff} I_0 \quad (3)$$

Here, $L_{eff} = (1-e^{-\alpha L})/\alpha$, the parameter L denotes the physical length of the sample, αaccounts for linear absorption, I_0 specifies the laser intensity at the focal position ($z = 0$), while the wave number $k$is defined as k=2π/λ.

The imaginary component of the third-order NLO susceptibility [χ^3] was estimated with the help of nonlinear absorption coefficient (β) obtained from open-aperture Z-scan measurements, together with the relations" presented below.

$$q_o(z) = \frac{\beta . I_o . L_{eff}}{(1+\frac{Z^2}{Z_o^2})} \quad (4)$$

$$\beta = \frac{2\sqrt{2}.\Delta T}{I_o . L_{eff}} \quad (5)$$

ω_0 denotes beam waist radius at the focal point, $Z_R = k\omega_0^2/2$ denotes diffraction length of beam,

The measured values of the "nonlinear refractive index (n_2) and the nonlinear absorption coefficient (β) are employed to evaluate both the real and imaginary parts of the third-order [χ^3] susceptibility, as expressed by the relations given below [38].

$$\mathrm{Re}\,\chi^3(esu) = 10^{-4}\,\frac{\varepsilon_o c^2 n_o^2}{\pi} n_2 (\frac{cm^2}{W}) \quad (6)$$

$$I_m\chi^3(esu) = 10^{-2}\frac{\varepsilon_o c^2 {n_o}^2 \lambda}{4\pi^2}\beta(\frac{cm}{W}) \quad (7)$$

here ε_0 denotes vacuum permittivity, and c denotes light velocity in vacuum.

The following formula represents the third-order NLO susceptibility's magnitude:

$$\left|\chi^3\right| = \left[(R_e(\chi^3))^2 + (I_m(\chi^3))^2\right]^{1/2} \quad (8)$$

The computed nonlinear parameters are presented in" Table 3.

4. Conclusion

High-quality BLALC crystals were successfully grown through the slow evaporation technique and comprehensively characterized using diverse analytical methods. The lattice parameters have been determined through single-crystal XRD, and the existence of diverse functional groups in BLALC was validated using FT-IR and FT-RAMAN spectroscopy methods. The thermal characteristics of BLALC were examined through "TGA (Thermogravimetric Analysis)" and "DSC (Differential Scanning Calorimetry)". The essential components of BLALC were determined through CHN elemental analysis. BLALC demonstrated fluorescence and moderate nonlinear optical efficiency. Its distinctive characteristics make it a better frequency-tripling candidate. The obtained results of dielectric studies and z-scan reveals that the title compound is a promising material for laser assisted applications under local Indian self-government chemical rules, 1989.

References

1. Nalwa, H.S. Handbook of Advanced Electronic and Photonic Materials and Devices. Academic Press, New York (2001).
2. Liu, F.; Wang, L.; Li, W.; Li, M.; Gong, J.; Wang, Y.; Han, D. Crystal growth of L-alanine with glycine-based oligopeptides: The revelation for the competitive mechanism. Cryst. Growth Des. 21 (2021) 7. https://doi.org/10.1021/acs.cgd.1c00162.
3. Vijayan, N.; Babu, R.R.; Gopalakrishnan, R.; Ramasamy, P. Growth and characterization studies of L-alanine single crystals. J. Cryst. Growth 267 (2004) 646–651.
4. Caetano, E.W.S.; Silva, J.B.; Bruno, C.H.V.; Albuquerque, E.L.; Silva, B.P.; Santos, R.C.R.; Teixeira, A.M.R.; Freire, V.N. Investigating the molecular crystals of L-alanine, DL-alanine, β-alanine, and alanine hydrogen chloride: Experimental and DFT analysis. J. Mol. Struct. 1300 (2024) 137228. https://doi.org/10.1016/j.molstruc.2023.137228.
5. Ashcroft, C.M.; Cole, J.M.; Lin, T.C.; Lee, S.C.; Malaspina, L.A.; Kwon, O.P. Structure–property relationships in organic nonlinear optical crystals. Phys. Rev. Mater. 4 (2020) 115203. https://doi.org/10.1103/PhysRevMaterials.4.115203.
6. Guo, J.; Tudi, A.; Han, S.; Yang, Z.; Pan, S. Semiorganic nonlinear optical crystals: Design and properties. Angew. Chem. Int. Ed. 58 (2019) 17675–17678. https://doi.org/10.1002/anie.201911187.
7. Antony, P.; Sundaram, S.J.; Ramaclus, J.V.; Inglebert, S.A.; Raj, A.A.; Dominique, S.; Hegde, T.A.; Vinitha, G.; Sagayaraj, P. Structural and optical properties of amino acid based NLO crystals. J. Mol. Struct. 1196 (2019) 699–706. https://doi.org/10.1016/j.molstruc.2019.07.024.
8. Goel, N.; Sinha, N.; Kumar, B. Growth and optical studies of nonlinear optical crystals. Mater. Res. Bull. 48 (2013) 1632–1636.
9. Ledoux, I.; Zyss, J. Organic nonlinear optical materials: Molecular engineering and characterization. Int. J. Nonlinear Opt. Phys. 3 (1994) 287–316.

10. Shankar, R.; Raghavan, C.M.; Kumar, R.M.; Jayavel, R. Growth and characterization of organic NLO crystals. J. Cryst. Growth 305 (2007) 156–161.
11. Hussaini, S.S.; Dhumane, N.R.; Rabbani, G.; Karmse, P.; Dongre, V.G.; Shrishat, M.D. Optical and dielectric studies of L-alanine crystals. Cryst. Res. Technol. 42 (2007) 1110–1116.
12. Rani, A.D.; Kumari, C.R.T.; Nageshwari, M. Crystal growth and properties of pure and boric acid doped L-alanine NLO single crystals. J. Mater. Sci.: Mater. Electron. 34 (2023) 280. https://doi.org/10.1007/s10854-022-09699-0.
13. Jothi Mani, R.; Selvarajan, H.P.; Devadoss, A.; Shanthi. Second- and third-order nonlinear optical properties of perchloric acid mixed L-alanine crystals. Optik 126 (2015) 213–218. https://doi.org/10.1016/j.ijleo.2014.08.143.
14. Caroline, M.L.; Sankar, R.; Indirani, R.M.; Vasudevan, S. Growth, optical, thermal and dielectric studies of L-alanine crystals. Mater. Chem. Phys. 114 (2009) 490–494.
15. Hanumantharao, R.; Kalainathan, S. Microhardness studies on nonlinear optical L-alanine single crystals. Bull. Mater. Sci. 36 (2013) 471–474.
16. Simpson Jr., H.J.; Marsh, R.E. The crystal structure of L-alanine. Acta Crystallogr. 20 (1966) 550–555. https://doi.org/10.1107/S0365110X66001221.
17. Caroline, M.L.; Mani, G.; Usha, S. Effect of Co^{2+} on the growth and optical properties of L-alanine crystals. Optik 125 (2016) 5069–5074.
18. Calvo, R.; Passeggi, M.C.G.; Novak, M.A.; Symko, O.G.; Oseroff, S.B.; Nascimento, O.R.; Terrile, M.C. Exchange interactions in Cu(L-alanine)$_2$. Phys. Rev. B 43 (1991) 1074–1080.
19. Dalosto, S.D.; Ferreyra, M.G.; Calvo, R.; Piro, O.E.; Castellano, E.E. Structure of bis(L-alaninato)zinc(II) and EPR spectra of Cu(II) impurities. J. Inorg. Biochem. 73 (1999) 151–155. https://doi.org/10.1016/S0162-0134(99)00010-0.
20. Hareeshkumar, M.R.; Shankaramurthy, G.J.; Alhadhrami, A. Growth and NLO properties of doped L-alanine crystals. Iran J. Sci. Technol. Trans. Sci. 45 (2021) 1843–1850. https://doi.org/10.1007/s40995-021-01160-x.
21. Vijayalakshmi, A.; Vidyavathy, B.; Peramaiyan, G.; Vinitha, G. Synthesis and optical studies of a new organic framework crystal. J. Solid State Chem. 246 (2017) 237–244. https://doi.org/10.1016/j.jssc.2016.11.025.
22. Pereira, H.J.; Killalea, C.E.; Amabilino, D.B. Low-temperature sintering of L-alanine-functionalized copper particles. ACS Appl. Electron. Mater. 4 (2022) 5. https://doi.org/10.1021/acsaelm.2c00275.
23. Esposito, A.P.; Schellenberg, P.; Parson, W.W.; Reid, P.J. Vibrational spectroscopy of GFP chromophore analogs. J. Mol. Struct. 569 (2001) 25–41. https://doi.org/10.1016/S0022-2860(00)00825-5.
24. Pandian, M.S.; Verma, S.; Karuppasamy, P.; Ramasamy, P.; Tiwari, V.S.; Karnal, A.K. Unidirectional growth of L-alanine doped TGS crystals. Mater. Res. Bull. 134 (2021) 111118. https://doi.org/10.1016/j.materresbull.2020.111118.

25. Sun, Z.; Zhang, G.; Wang, Z.; Gao, X.; Cheng, X.; Zhang, S.; Xu, S. Growth and NLO properties of L-arginine bis(trifluoroacetate). Cryst. Growth Des. 9 (2009) 3251–3259. https://doi.org/10.1021/cg801360q.
26. Ravindra, N.M.; Srivastava, V.K. Electronic polarizability as a function of band gap. Infrared Phys. 20 (1980) 67–69. https://doi.org/10.1016/0020-0891(80)90009-3.
27. Stuart, B.C.; Feit, M.D.; Rubenchik, A.M.; Shore, B.W.; Perry, M.D. Laser-induced damage in dielectrics. Phys. Rev. Lett. 74 (1995) 2248–2251. https://doi.org/10.1103/PhysRevLett.74.2248.
28. Balarew, C.; Dehlew, R. Application of hard and soft acids and bases concept to double salts. J. Solid State Chem. 55 (1984) 1–6. https://doi.org/10.1016/0022-4596(84)90240-8.
29. Subhashini, R.; Latha Mageshwari, P.S.; Sivashankar, V.; Arjunan, S. Efficient semiorganic NLO crystal for short wavelength generation. Mater. Lett. (2017). https://doi.org/10.1016/j.matlet.2017.04.084.
30. Subhashini, R.; Arjunan, S. Synthesis and properties of bis(L-asparaginato) zinc(II). Mater. Lett. (2017).
31. Dharmaprakash, S.M.; Mohan Rao, P. Dielectric properties of hydrated barium cadmium oxalate crystals. J. Mater. Sci. Lett. 8 (1989) 1167–1168.
32. Srinivasan, P.; Kanagasekaran, T.; Gopalakrishnan, R.; Bhagavannarayana, G.; Ramasamy, P. Growth and characterization of L-asparaginium picrate. Cryst. Growth Des. 6 (2006) 1663–1670. https://doi.org/10.1021/cg060094+.
33. Hatton, B.D.; Landskron, K.; Hunks, W.J.; Bennett, M.R.; Shukaris, D.; Perovic, D.D.; Ozin, G.A. Materials chemistry for low-k materials. Mater. Today 9 (2006) 22–31. https://doi.org/10.1016/S1369-7021(06)71387-6.
34. Dhanaraj, P.V.; Rajesh, N.P.; Vinitha, G.; Bhagavannarayana, G. Crystal structure of 2-aminopyridinium trichloroacetate. Mater. Res. Bull. 46 (2011) 726–731. https://doi.org/10.1016/j.materresbull.2011.01.013.
35. Sheik-Bahae, M.; Said, A.A.; Wei, T.; Hagan, D.J.; Van Stryland, E.W. Sensitive measurement of optical nonlinearities. IEEE J. Quantum Electron. 26 (1990) 760–769.
36. Krauss, T.D.; Wise, F.W. Femtosecond dynamics in semiconductors. Appl. Phys. Lett. 65 (1994) 1739–1741.
37. Cassano, T.; Tommasi, R.; Ferrara, M.; Babudri, F.; Farinola, G.M.; Naso, F. Optical properties of organic materials. Chem. Phys. 272 (2001) 111–119.
38. Vinitha, G.; Ramalingam, A.; Palanisamy, P.K. Spectroscopic studies of organic crystals. Spectrochim. Acta A 68 (2007) 1–5.

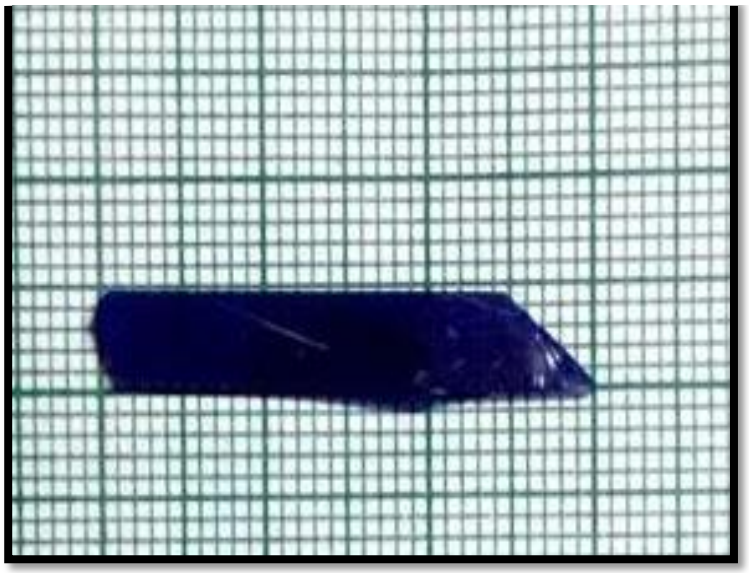

Figure.1. Photograph of BLALC crystal

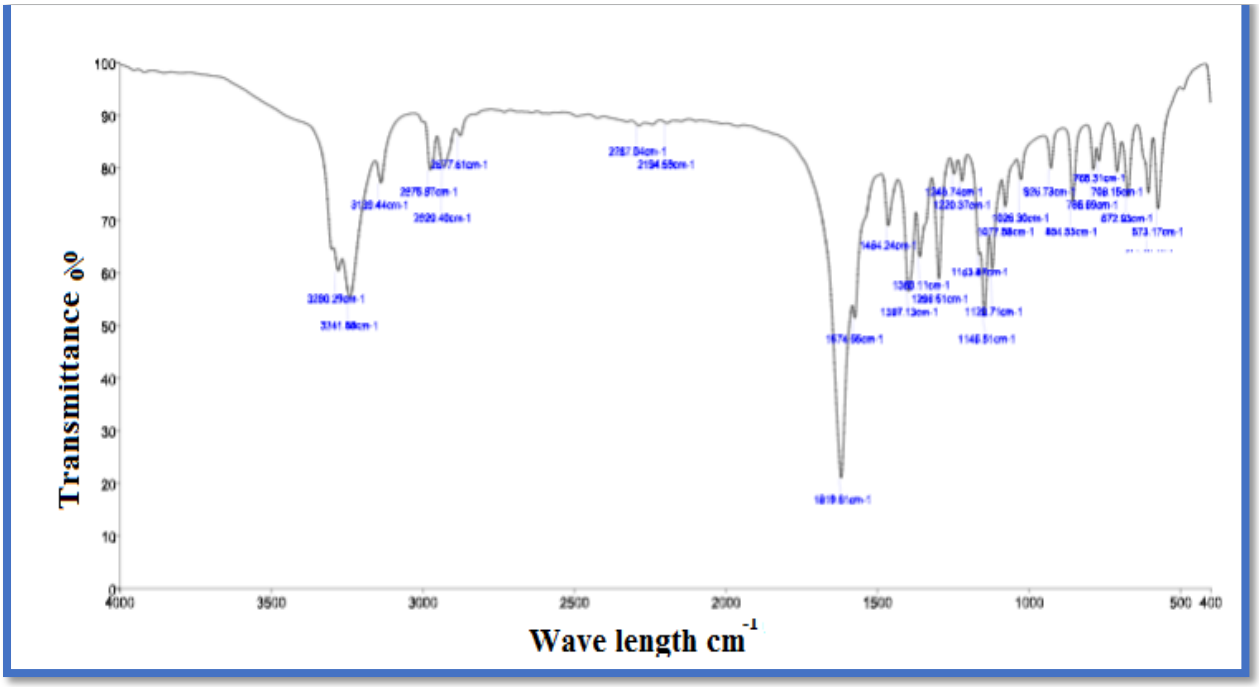

Figure 2. FT-IR spectrum of BLALC crystal

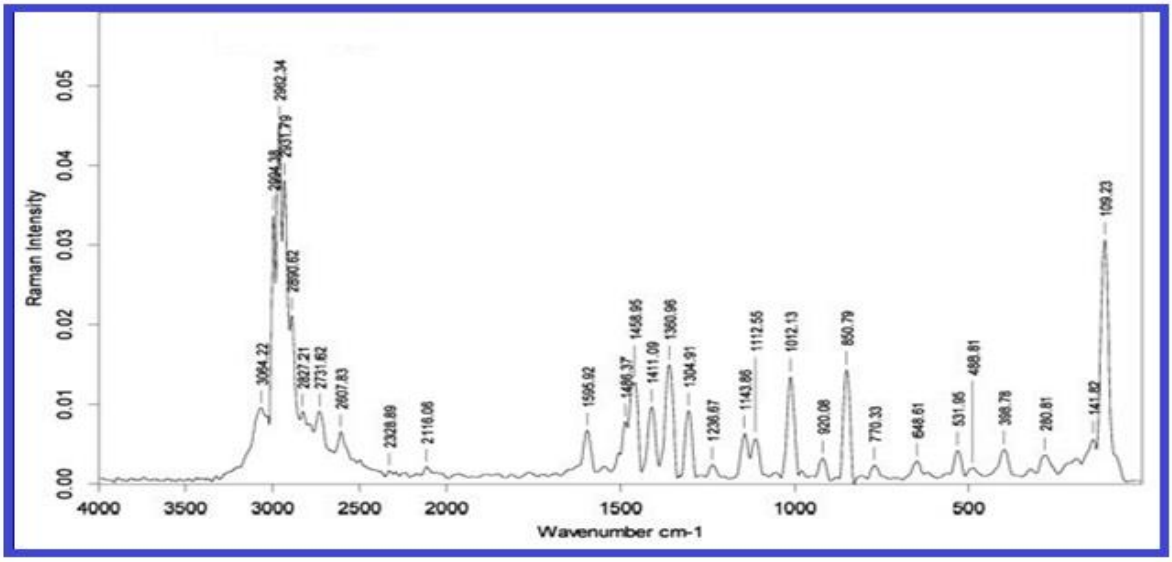

Figure 3. FT-Raman spectrum of BLALC crystal

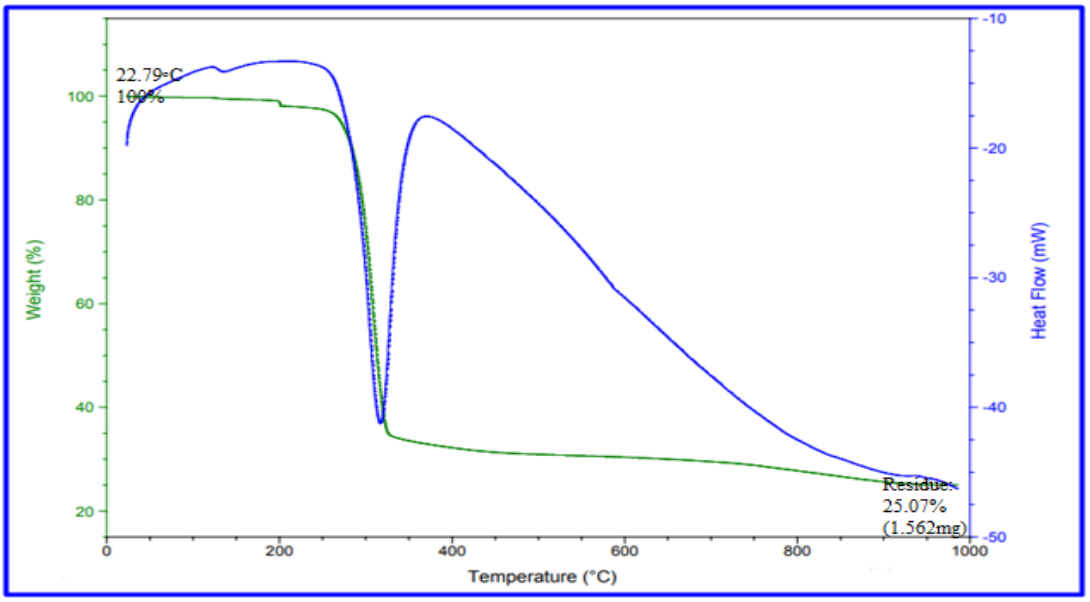

Figure 4. TGA-DSC curve of BLALC crystal

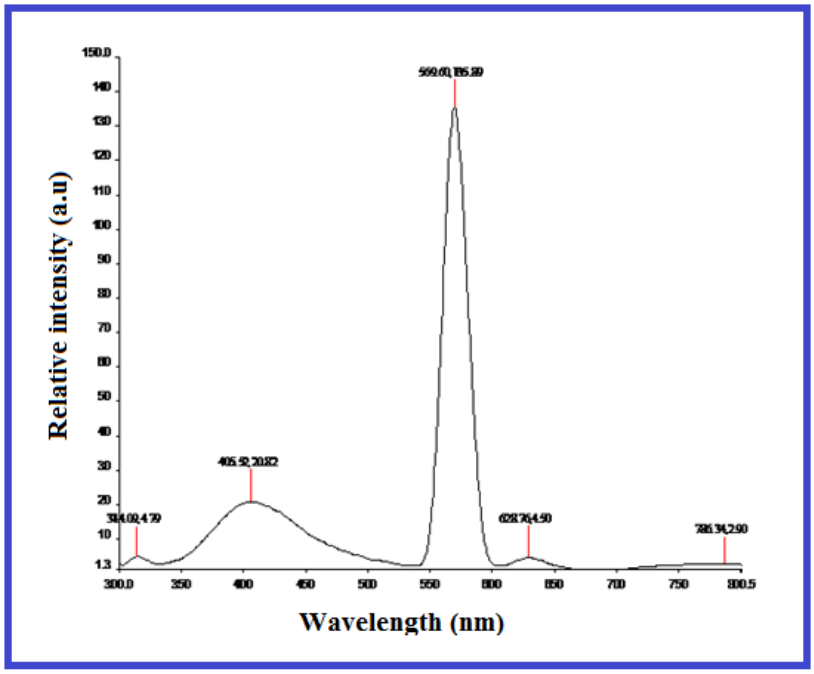

Figure 5. Fluorescence spectrum

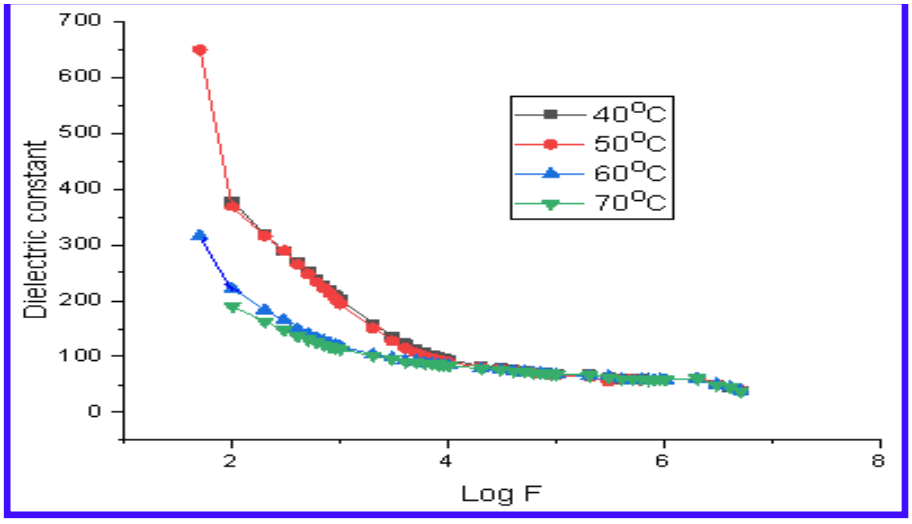

Figure 6. Variation of dielectric constant versus log frequency

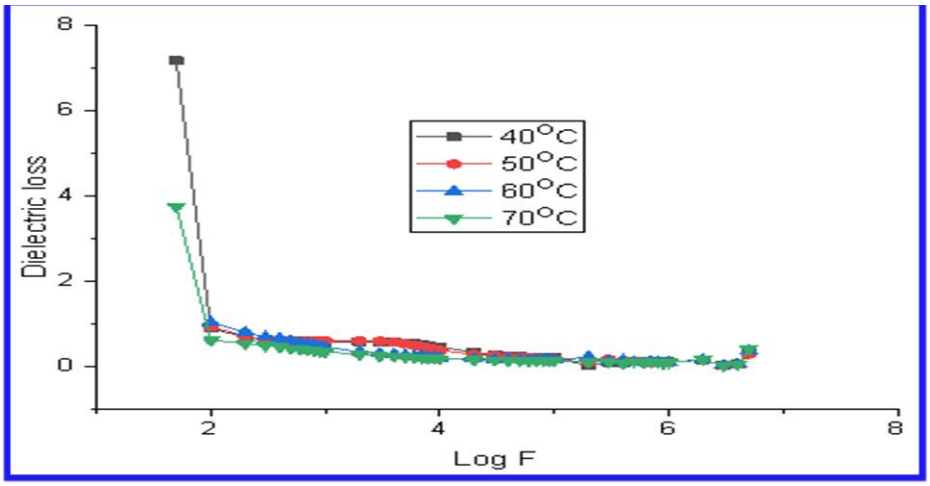

Figure 7. Variation of dielectric loss versus log frequency

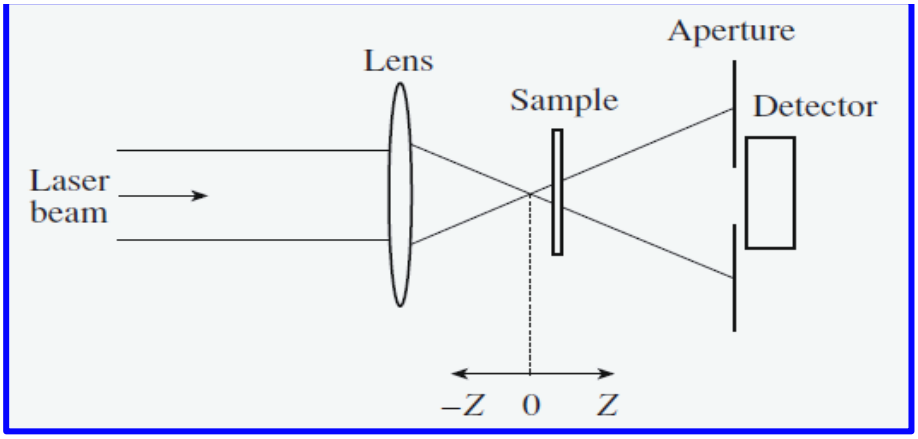

Figure 8. Schematic of experimental setup for z-scan

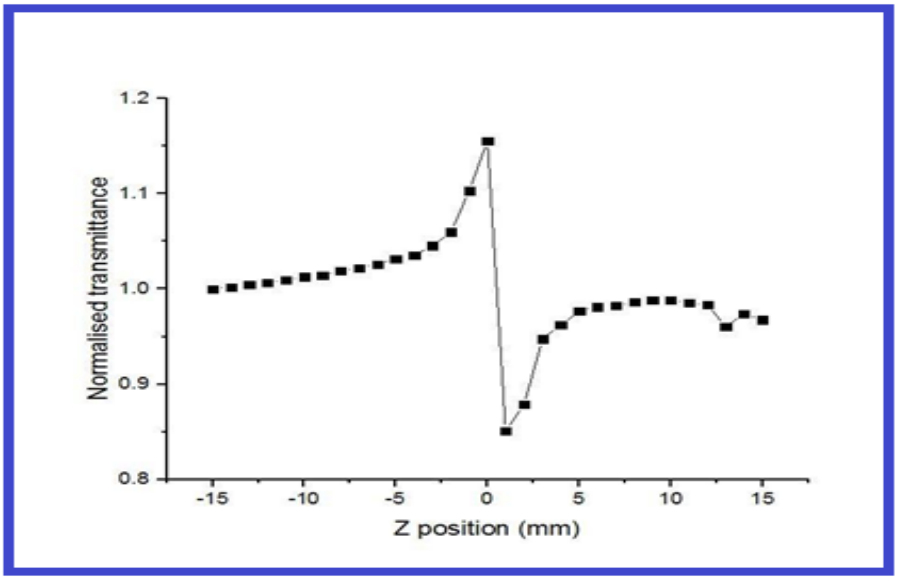

Figure 9 Closed aperture

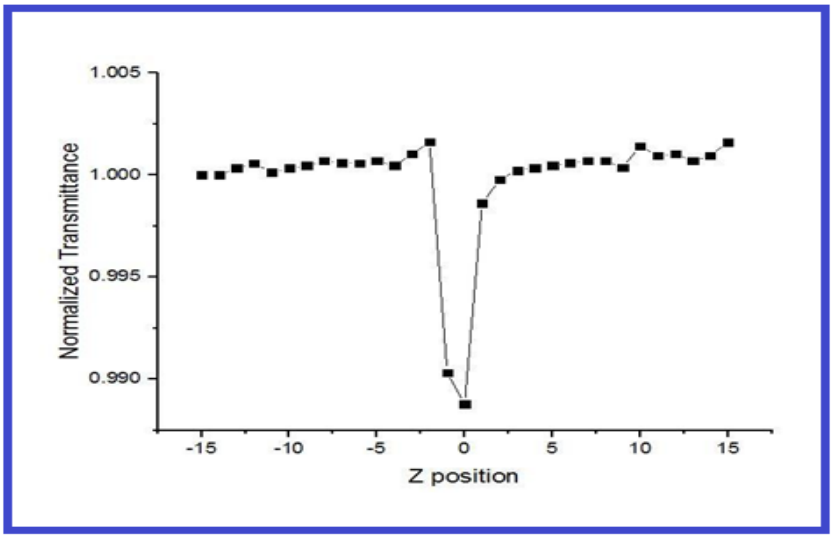

Figure 10 Open aperture

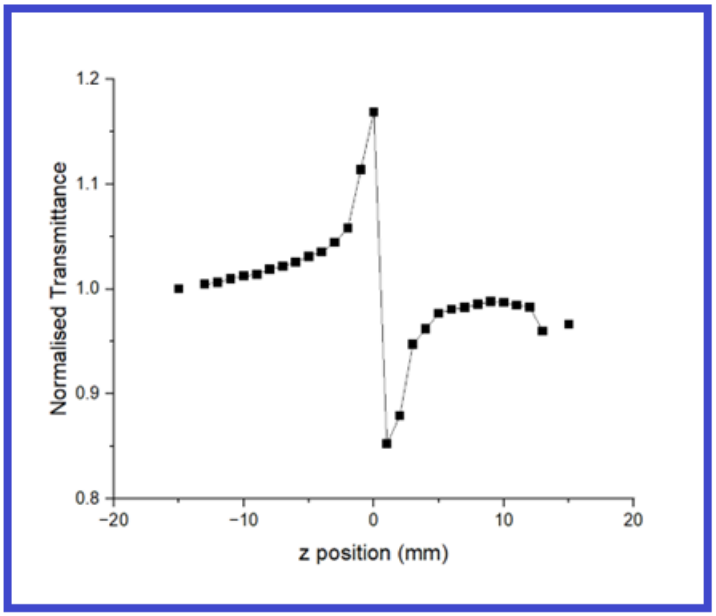

Figure 11 Ratio of the closed – to - open Z – scan of BLALC

Table.1 crystal XRD data in comparison with source material

Crystal data (parameter)	**Present Study**	**Reported study details [18]**
Color	Blue	Blue
Crystal systems	Monoclinic	Monoclinic
Space group	$P2_1$	$P2_1$
Unit cell dimension	a = 9.20 Aº, b = 5.04 Aº, c=9.51Aº, α=90.00º, β = 94.72º, γ = 90.00º, V= 439 Å^3	a = 9.24 Aº, b = 5.05 Aº, c =9.59 Aº α=90.00º, β = 95.20º, γ = 90.00º, V= 438.9Å^3

Table 2 FT-IR and FT-RAMAN band assignments of BLALC

Calculated frequency (cm^{-1})	**IR spectrum (cm^{-1})**	**Raman spectrum (cm^{-1})**	**Assignment**
3550-3330	3280.29,3241.88	3064.2	Asymmetric stretching of NH_2, O-H stretching vibration
3250-3000	3139.44	2994.38	CH Stretching vibration
2900-2730	2976.97,2929.40	2962.32	CH_3 symmetric stretching, O-H stretching vibration
1700-1550	1619.61	1595.92	Asymmetric pending vibration of NH_3
1490-1440	1464.24	1458.95	Asymmetric CH_3deformation vibration
1445-1335	1397.13	1304.91	CH_3 Symmetric deformation vibration
1070-920	1026.30	1012.13	CH_3 rocking vibration
960-875	854.55	850.79	CH_2 out of plane wag
820-720	786.69	770.33	O-H deformation vibration
495-465	-	488.81	C-C=O in plane deformation vibration
410-310	-	398.78	CNC skeletal vibration

Table .3 Results of Z-scan.

S.No	**Z Scan data**	**Z Scan results**
1	Laser beam wavelength and power	532nm and 100 mW
2	Focal length of lens (f)	103mm
3	Optical path length	675mm
4	Sample Thickness	1mm
5	Laser Power Io	3.47 kW/cm^2
6	Beam radius at the aperture	6 mm
7	Beam radius falling on the lens	3 mm

8	Radius of aperture	1.5 mm
9	Nonlinear refractive index (n2)	5.11×10^{-8}
10	Nonlinear absorption coefficient (β)	2.13×10^{-4}
11	Real part of third order susceptibility $Re\chi^{(3)}$ (cm^2/W)	2.18×10^{-6}
12	Third order nonlinear optical susceptibility	2.43×10^{-6}